THE JOURNAL OF THE ACOUSTICAL SOCIETY OF KOREA Vol.20, No.1E 2001. 3. pp. 31~37

A Study on the Effects of Parameter Sensitivity on Matched Field Processing

Cheolsoo Park*, Woojae Seong*, Hang-Soon Choi*, Kyu-Yeul Lee*

*Dept. of Ocean Engineering, Seoul National Univ.
(Received 11 December 2000 ; accepted 1 February 2001)

Abstract

Matched Field Processing (MFP) is a successive process of correcting mismatches between true and assumed parameters by matching the measured acoustic field data with numerically simulated data which we call replica. The MFP is widely used both in geo-acoustic parameter inversions and in source localizations. Whether a certain parameter can be inverted effectively or whether a source can be localized correctly depends on the amount of the influence that a parameter has on the acoustic field during the matching process. Sensitive parameters can be better estimated than the less sensitive ones in MFP. On the contrary, the sensitive parameters affect adversely on the source localization results when they have uncertainties. In this paper, a sensitivity index is defined based upon the field variation resulting from the perturbed parameters. Numerical test results show that the index behaves in accordance with the results of source localization under a mismatched environment and also with the inversion solutions.

Keywords *: MFP, Sensitivity index, Source localization, Inversion*

I. Introduction

Matched Field Processing (MFP) is a successive process to correct mismatches between true and assumed paramenters by matching the measured acoustic field data with numerically simulated data which we call replica. The MFP is widely used both in geo-acoustic parameter inversions and in source localizations [1,2,3].

The MFP utilizes the full acoustic field structure that is formed under complicated processes including interactions between sound sources and the environmental parameters.

Corresponding author: Woojae Seong(wseong@snu.ac.kr)
Seoul National University, Seoul 151-742, Korea

The acoustic field can be affected significantly by some parameters while it can be unaffected by others. As an example, the acoustic field of a water column shows considerable variability by the sound speed fluctuation due to internal waves[4]. But a density change in the deep bottom can make little influence on the sound structure of the water column. Therefore, the sensitivity of a parameter can be referred to as an amount of effects made on the acoustic field by the parameter.

Since the parameter sensitivity plays an important role in the MFP, many efforts have been made on researches related to the sensitivity both in the source localizations [5,6,7,8] and in geo-acoustical parameter inversions[9,10]. The sensitivity study in the source localization is mainly dealt with environmental mismatches and robustness of processors. In general, the sensitive parameters in a given environment affect adversely on the source localization results when they have uncertainties. In the geo-acoustical parameter inversion, the sensitivity is usually referred to as the ambiguity of the estimation of the parameters. Many inversion schemes utilize the sensitivities of the parameters to be inverted. Ainslie et al.[9] proposed an iterative scheme based on the parameter sensitivities, and Fallat et al.[10] excluded the insensitive parameters in their inversion.

In the papers mentioned above, the sensitivities are given heuristically. Therefore, it is useful to develop a method which can define the sensitivities quantitatively.

In this paper, a sensitivity index is defined using an acoustic field perturbation due to the change of a parameter. Numerical test results are shown for (1) the source localization tests under environmental mismatches and (2) the geo-acoustical inversion tests along with the sensitivity indexes of the various parameters.

II. Sensitivity index

The acoustic field is, in general, a function of environmental parameters, m_i' s, which are represented by a vector $\boldsymbol{m}_0 = [m_1, m_2, \cdots, m_i, \cdots, m_N]^T$, where N is the number of parameters. If there occurs a small change in a certain parameter, m_i , then the perturbed acoustic field can be expressed by,

$$p(m_1, \cdots, m_i + \triangle m_i, \cdots, m_N) = p(\boldsymbol{m}_o) + \triangle m_i \frac{\partial p(\boldsymbol{m}_o)}{\partial m_i} + \varepsilon. \tag{1}$$

The approximation error ε is assumed to be small compared with the original field.

When w and s represent simulated and measured data respectively, Bartlett processor Φ_B becomes[1],

$$\Phi_B = \boldsymbol{w}^* \langle ss^* \rangle \boldsymbol{w}. \tag{2}$$

Here $\langle \cdot \rangle$ represents the ensemble mean and * denotes the conjugate transpose. The data s is composed of the signal s_o and noise $\boldsymbol{n}$, which is independent of the signal. Then the Bartlett power can be written as,

$$\Phi_B = \boldsymbol{w}^* s_o s_o^* \boldsymbol{w} + \boldsymbol{w}^* \langle \boldsymbol{n}\boldsymbol{n}^* \rangle \boldsymbol{w} = \Phi_o + \Phi_n. \tag{3}$$

Note that both the signal and the replica vectors are normalized such that $s_o * s_o = w * w = 1$. Assuming deterministic mismatches on parameters, we focus on the deterministic processor power Φ_o. Considering i-th parameter mismatch, the normalized processor power becomes

$$\Phi_m = \frac{\boldsymbol{w}^* \langle (s_o + \triangle s_i)(s_o + \triangle s_i)^* \rangle \boldsymbol{w}}{(s_o + \triangle s_i)^* (s_o + \triangle s_i)}, \tag{4}$$

where, s_o and $\triangle s_i$ are the original signal vector and the perturbed signal vector respectively.

After letting $\boldsymbol{w}$ be s_o and assuming $s_o^* \triangle s_i + \triangle s_i^* s_o + \triangle s_i^* \triangle s_i \ll 1$, eq.(4) can be approximated as,

$$\Phi_m \simeq 1 - (\triangle s_i^* \triangle s_i - s_o^* \triangle s_i \triangle s_i^* s_o). \tag{5}$$

The first term "1" on the right hand side of eq.(5) is the maximum Bartlett power, which happens when there are no mismatches and the second term is an error due to the parameter perturbation. Since the error term corresponds to the sensitivity of the parameter on the acoustic field, the sensitivity index $I(m_i)$ is defined as,

$$I(m_i) = \triangle s_i^* \triangle s_i - s_o^* \triangle s_i \triangle s_i^* s_o. \tag{6}$$

The degradation of the processor power depends on the angle deviation of the perturbed signal from the original signal as well as on the amplitude of the perturbed signal.

We note that the sensitivity indexes can be defined using various processors other than the Bartlett processor. However, the algebraic sensitivity index derivation is not trivial. Besides, the sensitivity index derived from the Bartlett power is representative of the general behavior of sensitivities of other processors.

III. Numerical tests

The original signal and the perturbed signal required by the sensitivity index in eq.(6) are obtained using the wavenumber integration technique[11]. The wave field satisfies the following linear equation,

$$[K]\{P\} = \{R\}. \tag{7}$$

In eq.(7), P is a pressure field vector, R is a source vector, and K is a global stiffness matrix composed of the Green's functions. After differentiating both sides of eq.(7) with respect to a parameter m_i and rearranging, we get another linear equation,

$$[K]\left\{\frac{\partial P}{\partial m_i}\right\} = \left\{\frac{\partial R}{\partial m_i}\right\} - \left\{\frac{\partial K}{\partial m_i}\right\}\{P\}. \tag{8}$$

From eq.(7) and eq.(8), the wave field $\{P\}$ and the differential wave field $\left\{\frac{\partial P}{\partial m_i}\right\}$ can be obtained in turn by inverting the stiffness matrix K. Finally, both the original signal and the perturbed signal are given as follows;

$$s = P/|P|, \tag{9}$$

$$\triangle s_i = \triangle m_i \frac{\partial P(m_o)}{\partial m_i} /|P|. \tag{10}$$

The change of the parameter $\triangle m_i$ should be small, and numerically we choose it as 0.1% of the parameter value.

3.1 Sensitivity index test

Numerical tests for the sensitivity index are performed for the environment given in Fig. 1 There are two seasonal cases, three array cases, and three frequency cases as shown in the legend included in the figure. Each case has 10 test parameters, whose number is denoted in brackets. Total of 252 trial sources are evenly distributed from 10m to 120m in depth and from 2.5km to 4.5km in range.

The test results are shown in Fig. 2 Although 252 sensitivity indexes are obtained from the tests for each parameter in each case, the distribution of the indexes are not informative. Instead, both the maximum and the mean index are shown in the figure.

Fig. 2(a) test was performed under the sound speed profile in summer and with 150 Hz source. The result of the test gives a typical tendency of the sensitivity for all 10 parameters. It is observed that all the parameters in the water column (parameter <1>,<2> and <3>) and some parameters (parameter <4> and <7>) in the top sediment layer have large sensitivity indexes. Especially, the P-wave speed of the top sediment layer shows remarkably large sensitivity. Fig. 2(b) test was performed in order to compare the effects of array position using 150 Hz source. There are no observable differences in mean values, but large sensitivity is observed in some regions under strongly downward refracting summer profile. Fig. 2(c) test was performed using different sources under the summer profile and sensitivities of P-wave speed and thickness of the top sediment layer are shown, respectively. The absolute value of the sensitivity index becomes larger as frequency gets higher. However, the relative ratio of sensitivity values between the two parameters does not change significantly as the frequency changes.

3.2 Source localization test

Source localization tests under environmental parameter mismatches are performed in order to observe the effects of the parameter sensitivity on the MFP.

The test environment is the same as the previous test except for the mismatched parameter. The mismatched parameter is chosen to be the P-wave speed of the top

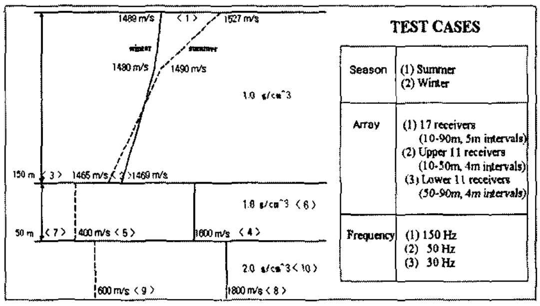

Figure 1. The sensitivity index test environment.

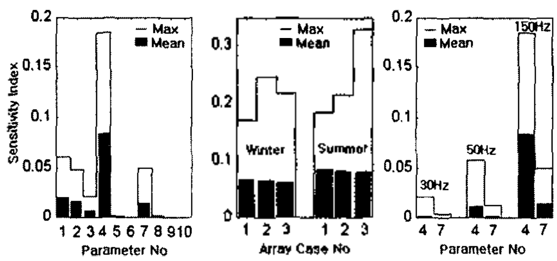

Figure 2. The sensitivity index test results.

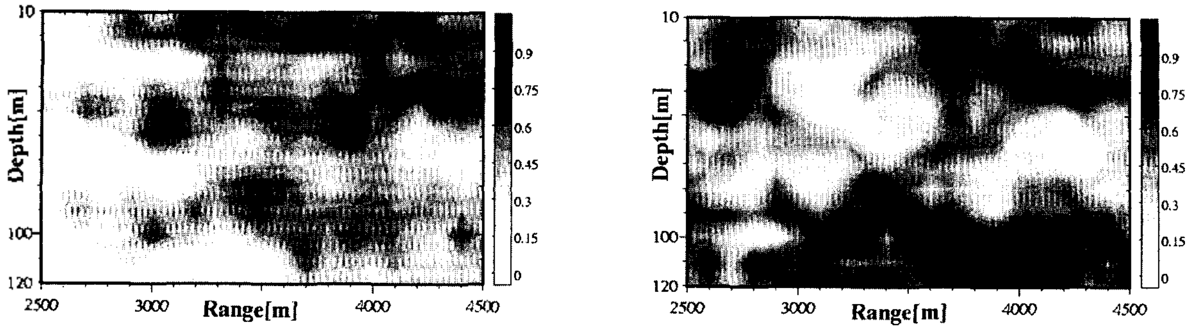

(a) sensitivity index (b) probability of failure

Figure 3. The source localization test results for 150Hz source.

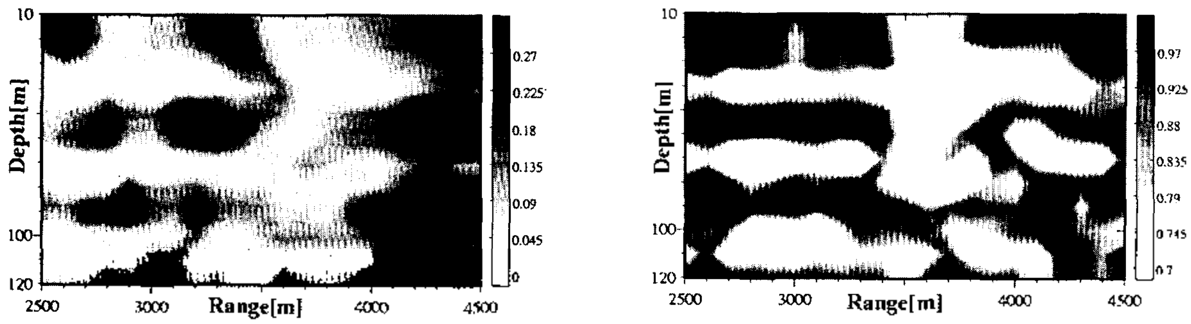

(a) sensitivity index (b) probability of failure

Figure 4. The source localization test results for 50Hz source.

sediment layer that showed the largest sensitivity. The value of the parameter is randomly selected within a bound between 1550m/s and 1650m/s. The tests are repeated 20 times for all source positions.

The sensitivity indexes are obtained and averaged during the source localization tests. In addition, a probability of failure is used for the source localization results which is compared with the sensitivity index. The probability of failure is defined as the ratio of the number of localization failure events over the total number of tests. The test is assumed to be a failure if the error between true and estimated source positions is over ±10m in depth and over ±100m in range.

The spatial distributions of sensitivities of the mismatched parameter are compared with the simulated source localization tests. A high frequency source (150Hz) and a low frequency source (50Hz) are separately used and the results are shown in Fig. 3 and Fig. 4, respectively. The contour level of (a) in figures is the sensitivity and that of (b) is the probability of failure in source localization.

Comparing Fig. 3(a) and Fig. 3(b) for the higher frequency source we observe that there are correspondences between the sensitivity and the probability of failure, especially in highly sensitive regions. With the lower frequency source in Fig. 4, the overall localization results are worse than that of the higher frequency, which is mainly due to the lack of modes in the acoustic field. Even in this case, slight agreements between sensitivities and

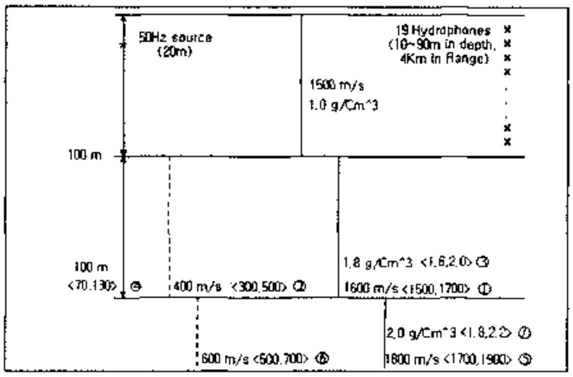

Figure 5. The inversion test environment.

Table 1. The inversion result.

Parameter No.	True	Best	Mean	Standard Deviation	Sensitivity Index
1	1600	1599.2	1598.3	0.013	1.92e-2
2	400	474.8	446.1	0.183	1.17e-4
3	1.8	1.98	1.89	0.193	5.84e-6
4	100	99.3	98.6	0.054	2.17e-3
5	1800	1797.6	1790.0	0.077	6.39e-4
6	600	572.4	555.4	0.179	1.64e-6
7	2	2.07	2.05	0.284	6.42e-7

localizations are observed.

3.3 Geo-acoustic parameter inversion test

A geo-acoustic parameter inversion test is performed in order to observe the effects of the parameter sensitivity on the inversion process. The test environment is shown in Fig. 5 The environmental model is simplified relative to the previous source localization tests. Even though broadband sources and multiple line arrays can be used for the improvement of inversion results[2], we considered a single frequency source and a vertical line array. However, inversion results for this simplified model offer sufficient insights into the relationship between sensitivities and inversions.

Information of the water column is known *a priori*. Therefore, we have 7 inversion parameters and they include P-wave speeds, S-wave speeds, densities and the sedimentary layer thickness. The GA [12] is used as an optimization tool and a modified Bartlett processor is defined to be the objective function as follows;

$$\Phi_{object} = 1 - w^* \langle ss^* \rangle w. \tag{11}$$

In eq.(11), w and s are the replica and the measured

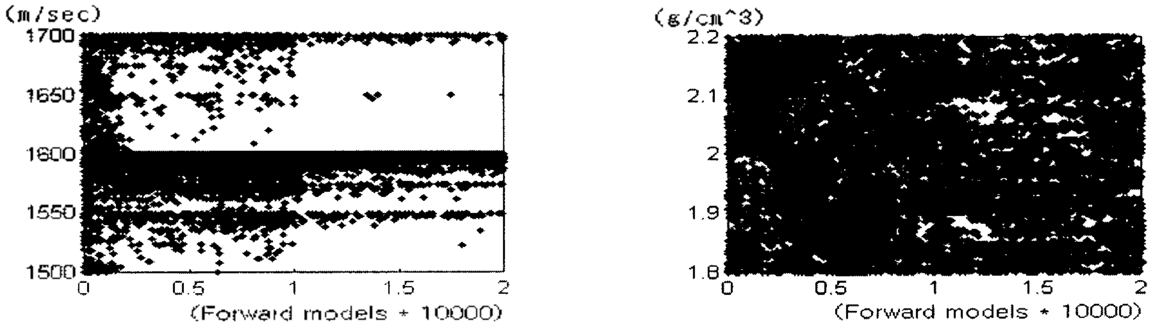

(a) P-wave speed of the top sediment layer

(b) density of the lower half space

Figure 6. The searching process.

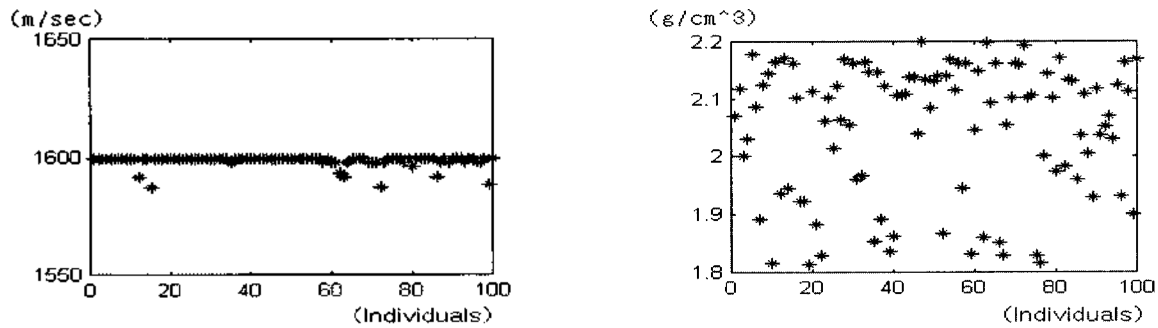

(a) P-wave speed of the top sediment layer

(b) density of the lower half space

Figure 7. The 100 best solutions.

data, respectively, and 10dB SNR white noises are added in the measured data. We choose the input parameters in the GA as follows: 100 individuals, 200 generations, cross-vers with probability 0.7 and mutations with probability 0.05. Possible test ranges are given in brackets of Fig.5 and each parameter has 128 search points.

Inversion results are given for the best solution, the mean solution of 100 best solutions, one standard deviation, and the sensitivity index. The standard deviations are normalized with respect to the pertinent test ranges. The sensitivity indexes are obtained at 200 random search points and are averaged.

Table 1 shows the inversion results. The results can be analyzed in view of the quality and the ambiguity of the solution. From the results, we can observe that both the best and the mean solutions are getting better as the sensitivity becomes higher, except for the parameter 7 which is the density of the lower half space. In addition, the standard deviations are strongly correlated with the sensitivity indexes. The standard deviation represents the ambiguity of the inversion solution.

Fig. 6 shows full searching processes for two extreme parameters. Fig. 6(a) is for the most sensitive parameter, i.e. the P-wave speed of the top sedimentary layer and Fig. 6(b) is for the least sensitive one, the density of the lower half space. A fast convergence toward a few good points is observed in Fig. 6(a). However, no convergence is observed in the insensitive case.

Fig. 7 shows the 100 best solutions in the order of fitness. The mean solutions with the standard deviations in Table 1 were obtained from the values in Fig. 7. All the solutions are concentrated on the true value in the sensitive case. On the other hand, the solutions of the insensitive parameter show a large scattering. It means that the parameter is too ambiguous to be estimated.

From the above discussions, it can be concluded that the more sensitive parameters can be estimated better in geo-acoustic inversions.

IV. Conclusion

We defined the sensitivity index that represents an amount of the influence made by a certain parameter on MFP results. The sensitivity index depends on the amplitude of the perturbed signal vector as well as on the angle deviation of the perturbed signal vector from the original signal vector.

The sensitivity indexes were calculated for the given environments. The environmental parameters pertinent to the water column and the top sedimentary layer showed large sensitivities.

The source localization tests under the environmental parameter mismatch showed correspondences between the sensitivity and the localization results, especially in the highly sensitive regions.

Finally, the geo-acoustic parameter inversion tests showed that the more sensitive parameters could be estimated better than the less sensitive ones both in terms of accuracy and ambiguity.

References

1. A.Tolstoy, *Underwater Acoustics* (World Scientific,Singapore, 1993).
2. A. Tolstoy, N. R. Chapman, and G. Brooke, Workshop 97 :Benchmarking for geoacoustic inversion in shallow water, *J. Computat. Acoust.*6(1&2),pp.1-28,1998.
3. A. B. Baggeroer, W. A. Kuperman, and P. N. Mikhalevski, An overview of matched field methods in ocean acoustics, *IEEE J. of Oceanic Eng.*18(4),pp.401-424,1993.
4. B. Choi, W. Seong, and J. Park, The Effect of Internal Waves on Acoustic Propagation, *J. Acoust. Soc. Kor.*19(5), pp.46-52,2000.
5. R. N. McDonough, Degraded performance of nonlinear array processors in the presence of data modeling errors, *J. Acoust. Soc. Am.*51,pp.1186-1193,1972.
6. C. Feuillade, D. R. DelBalzo, and M. M. Rowe, Environmental mismatch in shallow-water matched-field processing: Geoacoustic parameter variability, *J. Acoust. Soc. Am.*85, pp.2354-2364,1989.
7. A. Tolstoy, Sensitivity of matched field processing to sound-speed profile mismatch for vertical arrays in a deep water Pacific environment, *J. Acoust. Soc. Am.*85,pp.2394-2404, 1989.
8. D. F. Gingras, Methods for predicting the sensitivity of matched field processors to mismatch, *J. Acoust. Soc. Am.*86, pp.1940-1949,1989.
9. M. A. Ainslie, R. M. Hamson, G. D. Horsley, A. R. James, R. A. Laker, M. A. Lee, D. A. Miles, and S. D. Richards, Deductive multi-tone inversion of seabed parameters, *J. Computat. Acoust.*8(2),pp.271-284,2000.

10. M. R. Fallat, P. L. Nielsen, and S. E. Dosso, Hybrid geo-–acoustic inversion of broadband Mediterranean sea data, *J. Acoust. Soc. Am.* 107, pp.1967–1977, 2000.
11. F. B. Jensen, W. A. Kuperman, M. B. Porter, and H. Schmidt, *Computational ocean acoustics* (AIP Press, 1994).
12. D. E. Goldberg, *Genetic algorithms in search optimization, and machine learning* (Addison Wesley Longman, 1989).

[Profile]

• **Cheolsoo Park**

Cheolsoo Park received the B.S. and M.S. degrees in Naval Architecture and Ocean Engineering from Seoul National University in 1997 and 1999, respectively. Since 1999, he is working toward the Ph.D. degree at Seoul National University. His current research interests are in the area of geo-acoustical parameter inversion, matched field inversion and experimental acoustics.

• **Woojae Seong**

Prof. Woojae Seong was born in Seoul, Korea. He got his B.S. and M.S. from Seoul National University in 1982 and 1984, respectively and his Ph.D. from M.I.T. in 1990. Currently he is a Professor at Seoul National University. His current research interests are in the areas of acoustic propagation modeling, underwater acoustic inversion problems, structural acoustics, and underwater instrumentations.

• **HangSoon Choi**

Dr. Hang S. Choi was born in Seoul, Korea. He got his B.S. and M.S. from Seoul National University, Korea in 1970 and 1972, respectively majoring in Naval Architecture and Dr.-Ing. from Technical University of Munich, Germany in 1979. Since then he has worked at Seoul National University.

• **KyuYeul Lee**

Dr. Kyu-Yeul Lee was born in Korea. He got his B.S. from Seoul National University, Seoul, Korea majoring in Naval Architecture and his M.S. and Ph.D. in Naval Architecture, Technical University Hannover, Germany in 1975 and 1982, respectively. He currently serves as Professor in Naval Architecture and Ocean Engineering, Seoul National University, Seoul, Korea.